

## Effect of conduction electrons on the polarized Raman spectra of copper oxide superconductors

D. Reznik, M. V. Klein, W. C. Lee, and D. M. Ginsberg

*Department of Physics, University of Illinois, 104 South Goodwin Avenue, Urbana, Illinois 61801*

S-W. Cheong

*AT&T Bell Laboratories, Murray Hill, New Jersey 07974*

(Received 6 March 1992)

The line shape, laser-wavelength dependence, coupling to phonons, and doping dependence of the Raman continua in  $\text{YBa}_2\text{Cu}_3\text{O}_7$  single crystals differ for photons polarized parallel and perpendicular ( $ZZ$  geometry) to the Cu-O planes. The  $ZZ$  continuum in  $\text{YBa}_2\text{Cu}_3\text{O}_7$  can be accurately fit to a formula that describes scattering by a "dirty" free electron gas with frequency-independent damping. The doping dependence of the  $ZZ$  continuum appears to be consistent with electronic scattering. We have found evidence against scattering by conduction electrons being the origin of the plane-polarized continua in copper oxides: in  $\text{YBa}_2\text{Cu}_3\text{O}_7$  and in  $\text{Sm}_2\text{CuO}_4$  materials the  $a$ -axis-polarized continuum does not change much with doping (a continuum in the insulating phases is just as strong as in the superconductors), whereas ir reflectivity measurements show that the density of the electronic states is strongly affected by doping.

### I. INTRODUCTION

The Raman-scattering continuum observed in high-temperature superconductors is one of the anomalous properties of the normal state of these materials, and has been the focus of theoretical and experimental research.<sup>1-8</sup> Several theories have been proposed recently to explain the properties of the continuum.<sup>5-8</sup> We performed a detailed study of the doping, polarization, and laser frequency dependence of the continuum in  $\text{YBa}_2\text{Cu}_3\text{O}_{7-\delta}$  at room temperature and compared these results to theoretical predictions. Raman cross sections in the insulating  $\text{YBa}_2\text{Cu}_3\text{O}_{6.1}$  and  $\text{Sm}_2\text{CuO}_4$  were also compared.

### II. EXPERIMENT

The sample preparation is described in detail elsewhere.<sup>9</sup> The single crystals of  $\text{YBa}_2\text{Cu}_3\text{O}_{7-\delta}$  ( $T_c = 90, 66,$  and  $0$  K) were grown by a flux method using yttrium stabilized zirconia crucibles. Microanalysis of our crystals shows less than 12 ppm of Zr impurities. No other impurities were found. The transition widths of the  $T_c = 90$  K and  $T_c = 66$  K crystals in the magnetization data are  $\sim 1$  and  $\sim 2$  K, respectively.

The Raman-scattering measurements were made at 300 K with the sample in air. A lens focused a 15-mW laser beam on the sample to a circular spot of  $\sim 40$   $\mu\text{m}$  in diameter. Optics consisting of a collimating lens (an  $f/1.5$  85-mm camera lens) and a focusing lens (300-mm achromat) focused scattered light onto the entrance slit of a Spex "Triplemate" Raman spectrometer equipped with a multichannel, nitrogen-cooled,  $516 \times 516$  CCD camera detector. The spectra were corrected for the frequency-dependent efficiency of the spectrometer and detector. Chromatic aberration did not cause intensity loss in our spectra from defocusing at large frequency shifts because

we underfilled the entrance slit of the spectrometer with the laser spot image.

The spectra were corrected for optical absorption, transmission and refraction at the sample-air interface by multiplying them by the sum of the absorption coefficients and the square of the index of refraction, and dividing by the product of the transmission coefficients. The optical constants were obtained from polarized ir reflectivity and ellipsometry measurements.<sup>10</sup>

We neglected to make a correction for the sample and polarization dependence of the index of refraction in our previous publications.<sup>11,12</sup> This is the reason for the differences between the spectra presented in this paper and those previously published. However, these differences do not change the qualitative picture discussed in our previous work.

In all the figures the intensity is proportional to the energy cross section ( $d\sigma/d\omega$ ) per unit volume.

### III. ZZ vs PLANE-POLARIZED CONTINUA

The laser wavelength dependences of the  $XX$ ,  $YY$ , and  $ZZ$  continua of  $\text{YBa}_2\text{Cu}_3\text{O}_7$  are shown in Fig. 1. [Notation:  $XY$  means that incident photons are polarized along  $X$  and scattered along  $Y$ ;  $X$  is the  $a$  axis,  $Y$  is the  $b$  axis (Cu-O chain), and  $Z$  is the  $c$  axis.] Assignments of the phonon peaks below  $800$   $\text{cm}^{-1}$  have been made elsewhere.<sup>13</sup> We assign the peak at  $1000$   $\text{cm}^{-1}$  and a small bump at  $1500$   $\text{cm}^{-1}$  in  $ZZ$  geometry to second- and third-order scatterings from the  $A_g$  O(4) mode, respectively.

The  $XX$  and  $YY$  continua are nearly flat at the  $4579\text{-\AA}$  incident laser wavelength, and decrease with Raman shift at the longer laser wavelengths. The continuum intensity shows a weak resonant enhancement towards the ultraviolet (a factor of  $\sim 2$  from 1.9 to 2.7 eV). The  $ZZ$  continuum decreases rapidly with frequency shift above 1000

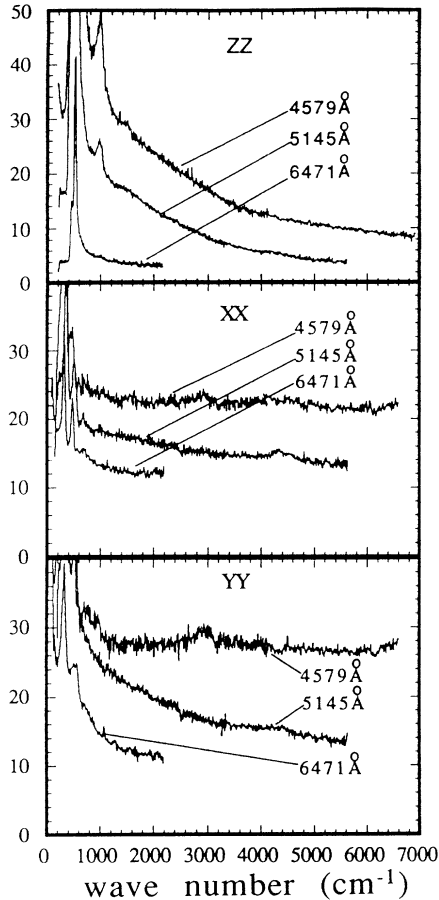


FIG. 1. Raman continuum in  $\text{YBa}_2\text{Cu}_3\text{O}_7$  in  $ZZ$ ,  $XX$ , and  $YY$  geometry at different laser wavelengths. Resolution  $\sim 50 \text{ cm}^{-1}$ . Intensity units for  $XX$  and  $YY$  are the same, but are different for  $ZZ$ .

$\text{cm}^{-1}$ , and its intensity shows a strong resonant enhancement towards the ultraviolet (a factor of  $\sim 7$  from 1.9 to 2.7 eV).

The line shape of the  $155\text{-cm}^{-1}$  mode is asymmetric in  $XX$  and  $YY$  geometries and symmetric in  $ZZ$  geometry.<sup>12–14</sup> The two continua must therefore be coupled differently to phonons in the two geometries.

It is difficult to identify the microscopic states responsible for the continuum because the scattering vertex is not known. But different resonant behavior, shape, interaction with phonons, temperature dependence,<sup>14</sup> and doping dependence (see the following sections) of the  $ZZ$  and plane-polarized continua point to a different microscopic origin of the continuum scattering in the two geometries.<sup>12</sup>

#### IV. ZZ CONTINUUM

We have used a “dirty” free-electron model, with frequency-independent damping (possibly due to impurities or phonons) for the electronic polarizability to analyze the scattering spectrum in  $ZZ$  geometry in  $\text{YBa}_2\text{Cu}_3\text{O}_7$ .<sup>15</sup> A calculation of Raman susceptibility, taking into account the electron self-energy as well as the

vertex corrections within the ladder approximation, gives the following expression<sup>15</sup>

$$\text{Im}(\chi) = \frac{\rho_0 \omega / \tau}{\omega^2 + (1/\tau)^2} \quad (1)$$

Figure 2 shows the  $ZZ$  continuum taken with laser wavelengths of 4579 and 5145-Å and fitted to Eq. (1) with two fitting parameters,  $\rho_0$  (amplitude) and  $1/\tau$  (assuming constant scattering rate—the same for the two curves). Above  $1000 \text{ cm}^{-1}$  the fit to the 4579-Å spectrum is very accurate, and the fit to the 5145-Å spectrum is less accurate, although still in quite good agreement with Eq. (1). Below  $1000 \text{ cm}^{-1}$  the same fit does not agree with the data because in this spectral shape the continuum is modified by the interaction with the  $500\text{-cm}^{-1}$  phonon.<sup>16</sup> The agreement of the spectra with the model is excellent at both incident laser wavelengths if the electron-phonon interaction is included (see inset). The value for the scattering rate  $1/\tau$  ( $700 \text{ cm}^{-1}$ ) was taken from the fit to the high-energy region. For the 4579-Å spectrum  $q$  was 3.59,  $\cos(\phi) = 0.38$  (in the notation of Ref. 16). Uncertainty in the value of  $1/\tau$  is around 30% because it is very sensitive to small changes in the spectral line shape (within experimental uncertainty). Since all the parameters in the fit to the low-energy part strongly depend on the value of  $1/\tau$ , their numerical values are accurate only to within an order of magnitude.

A good agreement of the experimental results with Eq. (1), derived for single-component intraband or interband scattering, suggests that the continuum observed in  $ZZ$  geometry is of electronic origin. We shall give the interpretation of these results within the local-density-approximation (LDA) picture, which has been used<sup>17</sup> to account for resonant behavior of phonons. Strong in-

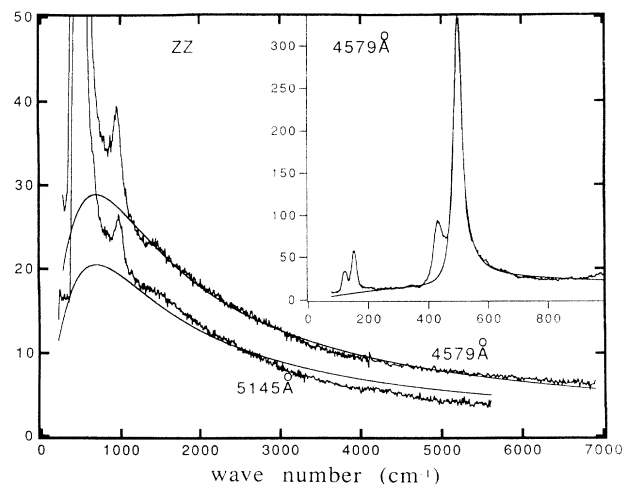


FIG. 2. Raman spectra in the  $ZZ$  geometry and 4579- and 5145-Å laser wavelengths fit to Eq. (1). The  $500\text{-cm}^{-1}$  phonon is truncated. The theoretical curves are represented by smooth lines. The inset shows a high-resolution low-energy  $ZZ$  spectrum, divided by the Bose factor  $[1+n(\omega)]$  to obtain  $\text{Im}(\chi)$ , taken with the 4579-Å laser wavelength, fit to  $500\text{-cm}^{-1}$  phonon interacting with the continuum described by Eq. (1). The 115-, 145-, and  $410\text{-cm}^{-1}$  phonons were not included in the fit.

teraction with the O(4) mode is suggestive of the bands involved in the scattering process. The two chain bands that cross the Fermi surface [O(4)(Z)-Cu(1)(Z<sup>2</sup>-Y<sup>2</sup>)-O(1)(Y) and O(4)(Y)-Cu(1)(XY)-O(1)(X)] interact strongly with the O(4) vibrations and could contribute excitations to the ZZ continuum.<sup>18</sup>

The frequency-independent scattering rate  $1/\tau$  could be caused by impurity<sup>15</sup> or phonon<sup>19</sup> scattering or both.<sup>19</sup> To the first approximation, spectral line shapes for optical-phonon scattering and for the impurity scattering are both described by Eq. (1) at frequencies much greater than phonon frequencies,<sup>19</sup> and are impossible to distinguish from the fit to the spectrum above 1000 cm<sup>-1</sup>. Below 1000 cm<sup>-1</sup>, where  $1/\tau$  is frequency dependent in the case of the phonon scattering and frequency independent in the case of the impurity scattering, Fano antiresonance of the 500-cm<sup>-1</sup> phonon introduces two extra fitting parameters, making a definitive analysis of the frequency dependence of  $1/\tau$  impossible.

If the above picture is correct, the continuum should vanish in the insulating phase YBa<sub>2</sub>Cu<sub>3</sub>O<sub>6+ $\delta$</sub>  (because it has neither chain bands nor a Fermi surface). For the insulating YBa<sub>2</sub>Cu<sub>3</sub>O<sub>6+ $\delta$</sub> , the continuum is absent in the ZZ geometry above 500 cm<sup>-1</sup> and the O(4) phonon lineshape is symmetric.<sup>20</sup> The ZZ spectrum of the insulating La<sub>2</sub>CuO<sub>4</sub> in Ref. 21 (Fig. 1) has no Raman continuum. Preliminary results show, however, that some continuum scattering is present in YBa<sub>2</sub>Cu<sub>3</sub>O<sub>6+ $\delta$</sub>  below 500 cm<sup>-1</sup>. This appears to be inconsistent with the intraband picture.<sup>22</sup> Further study of the intensity of the continuum in the YBa<sub>2</sub>Cu<sub>3</sub>O<sub>7- $\delta$</sub>  and other copper oxide families at different  $\delta$  in ZZ geometry is necessary to test this model.

## V. PLANE-POLARIZED CONTINUA

Raman spectra of YBa<sub>2</sub>Cu<sub>3</sub>O<sub>7- $\delta$</sub>  (YBCO) single crystals in XX, YY, XY, and YX scattering geometries were taken from *ab* faces of untwinned single crystals.

Figures 3 and 4 show spectra of an "as grown" insulating single crystal, an untwinned  $T_c = 66$  K single crystal (with reduced oxygen concentration) and an untwinned  $T_c = 90$  K single crystal. The results have been confirmed on other samples.

In agreement with previous work<sup>1,4</sup> we observe a strong two-magnon scattering peak at  $\sim 2700$  cm<sup>-1</sup> in the XX spectrum of the insulating sample. Our data do not confirm a previously reported result that two-magnon scattering exists in the oxygen reduced, superconducting  $T_c = 66$  K, samples.<sup>4</sup> A broad  $B_{1g}$  peak around 2500 cm<sup>-1</sup>, seen by Lyons *et al.*,<sup>4</sup> does not exist in our spectra. However, we have observed the two-magnon scattering three months after the original measurements. During this time the sample was kept in dry air. Oxygen depletion near the surface probably generated the two-magnon peak.

In addition to the two-magnon scattering,<sup>1</sup> a strong background continuum extending above 10 000 cm<sup>-1</sup> was also present in the insulating sample (see Fig. 5). The two-magnon scattering disappears with doping, but the continuum in XX geometry remains unchanged. The YY

continuum is stronger than the XX continuum in the superconducting crystals. The X-Y anisotropy is significantly greater in the oxygen deficient ( $T_c = 66$  K) sample than in the fully oxygenated ( $T_c = 90$  K) sample.

Figure 2 shows a comparison between the continua in the insulating YBa<sub>2</sub>Cu<sub>3</sub>O<sub>6.1</sub>, annealed in nitrogen for 48 h at 650 °C with a fast quench to 77 K, and in Sm<sub>2</sub>CuO<sub>4</sub>. The continuum is a factor of 2 weaker in Sm<sub>2</sub>CuO<sub>4</sub> below 1500 cm<sup>-1</sup> and is roughly the same as in YBa<sub>2</sub>Cu<sub>3</sub>O<sub>6.1</sub> above 6000 cm<sup>-1</sup>. The YBCO crystal used for Fig. 5 had a lower oxygen content than the as-grown crystal (Figs. 3 and 4), which resulted in a stronger and narrower two-magnon peak, but no change in the continuum.

The spectral line shape of the plane-polarized continua clearly does not fit a clean<sup>26</sup> or dirty<sup>15</sup> single-band model and nothing in the band-structure calculations<sup>18</sup> points to an interband scattering process, which would produce these spectra. However, the experimental data can be fit to the Eq. (1) reasonably well, if  $1/\tau$  is assumed to vary linearly with  $\omega$  (for example see Refs. 3 and 6). Since a similar frequency dependence of the scattering rate has also been observed in the ir conductivity, many theories of the Raman-continuum assume that it is caused by the scattering by the conduction electrons, observed by in-

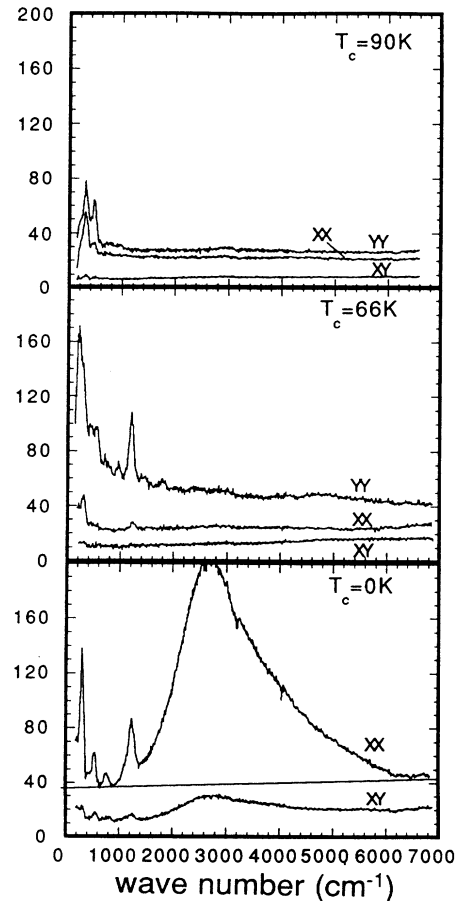


FIG. 3. High-resolution spectra of the continuum in the insulating and  $T_c = 90$  K single crystals. Resolution  $\sim 10$  cm<sup>-1</sup>. Intensity units are the same for all the spectra.

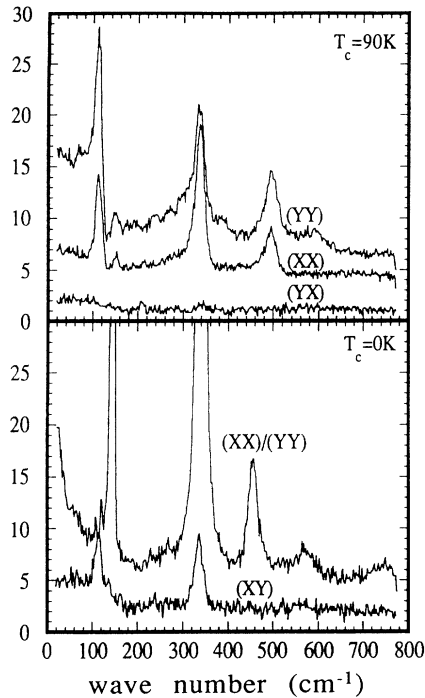


FIG. 4. The continuum in the insulating,  $T_c = 66$  and  $90$  K single crystals. Resolution  $\sim 50$   $\text{cm}^{-1}$ . Intensity units are the same (but different from Fig. 5). The horizontal line in the  $T_c = 0$  K graph is a guide for the eye representing the background continuum.

frared (ir) conductivity measurements.<sup>5-8</sup> If so, the doping and polarization dependence of the continuum and the ir conductivity should be similar. The experimental results below  $1$  eV in YBCO and  $\text{Sm}_2\text{CuO}_4$  materials can be summarized as follows (Refs. 10, 11, 13, and 23-26).

(1) The conductivity is an order of magnitude smaller in the insulating phases than in the metallic phases,<sup>10,23,26</sup> but the Raman continuum in the insulating phases is as strong as in the metallic ones.

(2) The room-temperature continuum in Ce-doped  $T'$  materials,<sup>25</sup> as well as in  $\text{La}_{2-x}\text{Sr}_x\text{CuO}_4$  (Fig. 5 in Ref. 21), does not change much as the two-magnon peak disappears with increased doping, but the ir conductivity has a strong doping dependence.<sup>26</sup>

(3) The integrated spectral weight of  $x$ -polarized conductivity below  $1$  eV is  $\sim 30\%$  greater in the YBCO  $T_c = 90$  K samples than in the  $T_c = 66$  K samples but the spectral weight of the  $XX$  Raman continuum is the same.

(4) The "chain contribution" to the conductivity in YBCO (defined as  $\sigma_{bb} - \sigma_{aa}$ ) is greater in  $T_c = 90$  K samples than in the  $T_c = 66$  K samples<sup>10</sup> but the opposite is true for the chain contribution to the Raman continuum (defined as the difference between  $YY$  and  $XX$  intensities).

So the intensity related properties of the ir conductivity and the Raman continuum are quite different.

Raman scattering and ir absorption can have different selection rules, so, they need not couple to the same electronic states.<sup>27</sup> But even if the Raman spectra reveal an

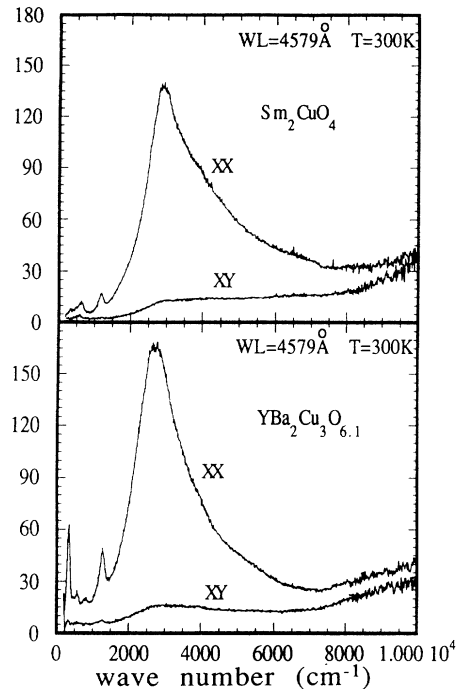


FIG. 5. Raman spectra of  $\text{Sm}_2\text{CuO}_4$  and  $\text{YBa}_2\text{Cu}_3\text{O}_{6.1}$ . Intensity units are the same (but different from Fig. 3).

electronic channel of a different symmetry than that of the ir spectra, we should still see zero scattering below the charge-transfer gap in the insulators, and an increase in  $XX$  and  $YY$  scattering as the carrier concentration increases with doping.

The major portion of the continuum intensity in the superconductors could be due to the scattering by conduction electrons only if the following were true.

(1) Photons couple to different continua of states in the insulating and metallic phases (for example localized states in the insulators and conduction electrons in the metals<sup>28</sup>), though there is no apparent change in the shape and intensity across the metal-insulator transition.

(2) The effective photon-continuum Raman coupling constant (the scattering vertex) increases in magnitude with decreasing carrier concentration in the metallic phases, resulting in a doping-independent  $XX$  continuum and a chain continuum weaker in the  $T_c = 90$  K than in the  $T_c = 66$  K YBCO crystals.

These coincidences do not seem very likely, especially since they have to hold for the  $\text{YBa}_2\text{Cu}_3\text{O}_{7-\delta}$  as well as for the  $\text{Sm}_2\text{CuO}_4$  (and maybe other) systems.

Although the entire continuum between  $0$  and  $1$  eV is unlikely to come from conduction electrons, it is possible that they contribute some intensity below  $0.1$  eV in the metallic phases and are responsible for the "gaplike" redistribution below  $T_c$  observed previously. Comparison of the temperature dependences of the continuum throughout the doping range is necessary to understand the role of conducting electrons at low energies. This work is currently under way.

## VI. CONCLUSIONS

We have found strong evidence that the microscopic origins of the ZZ and plane-polarized continua are different in YBCO. The ZZ continuum in  $\text{YBa}_2\text{Cu}_3\text{O}_7$  is a resonant Raman process, which can be accurately fit with single-band or interband models plus impurity scattering. Doping dependence of the plane polarized continua in  $\text{YBa}_2\text{Cu}_3\text{O}_7$  and  $\text{Sm}_2\text{CuO}_4$  materials is not consistent with scattering of light by the conduction electrons, and is quite different from the doping dependence of the ir conductivity.

## ACKNOWLEDGMENTS

A sample on which preliminary results on the ZZ scattering were obtained, was provided by B. W. Veal of Argonne National Laboratory. The authors are grateful to S. L. Cooper and A. L. Kotz for providing their data on the optical constants before publication. D. R. would also like to thank S. L. Cooper, R. Liu, and A. Zawadowski for helpful discussions. This project received support from the NSF under Contract No. DMR90-17156 and through the NSF-funded Science and Technology Center for Superconductivity under Contract No. DMR91-20000.

- 
- <sup>1</sup>S. Sugai, Y. Entomoto, and T. Murakami, *Solid State Commun.* **72**, 1193 (1989).
- <sup>2</sup>T. Staufner, R. Hackl, and P. Muller, *Solid State Commun.* **75**, 975 (1990).
- <sup>3</sup>F. Slakey, M. V. Klein, D. Reznik, J. P. Rice, D. M. Ginsberg, A. P. Paulikas, J. W. Downey, and B. W. Veal, *Proc. SPIE* **1336**, 86 (1990).
- <sup>4</sup>K. B. Lyons, P. A. Fleury, R. R. Singh, and P. E. Sulewski, *Proc. SPIE* **1336**, 66 (1990); R. P. Singh, *Comments Condens. Mater. Phys.* **15**, 241 (1991).
- <sup>5</sup>C. M. Varma, P. B. Littlewood, S. Schmidt-Rink, E. Abrahams, and A. E. Ruckenstein, *Phys. Rev. Lett.* **63**, 1996 (1989).
- <sup>6</sup>A. Virosztek and J. Ruvalds, *Phys. Rev. B* **45**, 347 (1992).
- <sup>7</sup>P. W. Anderson, *Physica C* **185-189**, 11 (1991).
- <sup>8</sup>B. S. Shastry and B. I. Shraiman, *Phys. Rev. Lett.* **65**, 1068 (1990).
- <sup>9</sup>J. P. Rice and D. M. Ginsberg, *J. Cryst. Growth* **109**, 432 (1991); W. C. Lee and D. M. Ginsberg, *Phys. Rev. B* **44**, 2815 (1991); G. H. Kwei, S-W. Cheong, Z. Fisk, F. H. Garson, J. A. Goldstone, and J. D. Thompson, *ibid.* **40**, 9370 (1989).
- <sup>10</sup>S. L. Cooper, A. L. Kotz, M. A. Karlow, M. V. Klein, W. C. Lee, J. Giapintzakis, and D. M. Ginsberg, *Phys. Rev. B* **45**, 2549 (1992).
- <sup>11</sup>D. Reznik, A. L. Kotz, S. L. Cooper, M. V. Klein, W. C. Lee, and D. M. Ginsberg, *Physica C* **185-189**, 1029 (1991).
- <sup>12</sup>D. Reznik, A. L. Kotz, S. L. Cooper, M. V. Klein, W. C. Lee, and D. M. Ginsberg, in *Proceedings of the International Workshop on Electronic Properties and Mechanisms of High  $T_c$  Superconductivity* (IWEPM), Tsukuba, Japan, 1991, edited by T. Ouchi, K. Kadowaki, and T. Sasaki, pp. 283-287 (North-Holland, Amsterdam, 1992).
- <sup>13</sup>K. F. McCarty, J. Z. Liu, R. N. Shelton, and H. B. Radousky, *Phys. Rev. B* **41**, 8792 (1990).
- <sup>14</sup>K. F. McCarty, J. Z. Liu, R. N. Shelton, and H. B. Radousky, *Phys. Rev. B* **42**, 9973 (1990); A. A. Maksimov, I. I. Tartakovskii, V. B. Timofeev, and L. A. Falkovskii, *Zh. Eksp. Teor. Fiz.*, **97**, 1047 (1990) [*Sov. Phys. JETP*, **70**, 588, (1990)].
- <sup>15</sup>M. Cardona and A. Zawadowski, *Phys. Rev. B* **42**, 10732 (1990).
- <sup>16</sup>U. Fano, *Phys. Rev.* **124**, 1866 (1961); F. Bechstedt and K. Peuker, *Phys. Status Solidi B* **72**, 743 (1975).
- <sup>17</sup>E. T. Heyen, S. N. Rashkeev, I. I. Mazin, O. K. Andersen, R. Liu, M. Cardona, and O. Jepsen, *Phys. Rev. Lett.* **65**, 3048 (1990).
- <sup>18</sup>O. K. Anderson, A. I. Liechtenstein, O. Rodrigues, I. I. Mazin, O. Jepsen, A. P. Antropov, O. Gunnarsson, and S. Gopalan, *Physica C* **185-189**, 147 (1991).
- <sup>19</sup>K. Itai, *Phys. Rev. B* **45**, 707 (1992).
- <sup>20</sup>D. Reznik *et al.* (unpublished).
- <sup>21</sup>S. Sugai, in *Mechanisms of High Temperature Superconductivity*, Springer Series in Material Science, Vol. 11, edited by H. Kamimura and A. Oshiyama (Springer-Verlag, Berlin, 1989).
- <sup>22</sup>R. Liu *et al.* (unpublished).
- <sup>23</sup>Z. Schlesinger, R. T. Collins, F. Hotzberg, C. Feild, S. H. Blanton, U. Welp, G. W. Grabtree, and Y. Fang, *Phys. Rev. Lett.* **65**, 801 (1990).
- <sup>24</sup>S. L. Cooper *et al.* (unpublished).
- <sup>25</sup>I. Tomeno, M. Yoshida, K. Ikeda, K. Tai, K. Takamuku, N. Koshizuka, S. Tanaka, K. Oka, and H. Unoki, *Phys. Rev. B* **43**, 3009 (1991).
- <sup>26</sup>S. Uchida, T. Ido, H. Takagi, T. Arima, Y. Tokura, and S. Tajima, *Phys. Rev. B* **43**, 7942 (1991).
- <sup>27</sup>M. V. Klein, in *Light Scattering in Solids I*, edited by M. Cardona (Springer, Berlin, 1983), Chap. 4.
- <sup>28</sup>S. L. Cooper (private communication).